Microscopic VECSEL Modeling

S. W. Koch*[a,b], J. Hader[b], J.V. Moloney[b]
[a] Department of Physics, Philips University Marburg, Renthof 5, 35032 Marburg/Germany; [b]College of Optical Sciences, University of Arizona, Tucson, AZ USA 85721

ABSTRACT

This tutorial gives an overview of the microscopic approach developed to describe equilibrium and nonequilibrium effects in optically excited semiconductor systems with an emphasis to the application for VECSEL modelling. It is outlined how nonequilibrium quantum theory is used to derive dynamic equations for the relevant physical quantities, i.e. the optically induced polarization and the dynamical carrier occupation probabilities. Due to the Coulombic many-body interactions, polarization and populations couple to expectation values of higher-order quantum correlations. With the help of a systematic correlation expansion and truncation approach, we arrive at a closed set of equations. Formally these can be combined with Maxwell's equations for the classical light field, yielding the Maxwell-semiconductor Bloch equations (MSBE). However, instead of the more traditional approach where losses and dissipative processes are treated phenomenologically and/or through coupling to external reservoirs, we derive fully microscopic equations for the carrier-carrier and carrier-phonon scattering as well as the effective polarization dephasing. Due to their general nature, the resulting equations are fully valid under most experimentally relevant conditions. The theory is applied to model the high-intensity light field in the VECSEL cavity coupled to the dynamics of the optical polarization and the nonequilibrium carrier distributions in the quantum-well gain medium.

Keywords: VECSEL modelling, nonequilibrium effects, microscopic theory, high power operation, short pulse operation

1. INTRODUCTION

An example for the schematic design of a VECSEL [1,2] is shown in Fig. 1. The main building block is the quantum-well (QW) gain material on top of the high-reflectivity Bragg mirror (DBR). Together, these constitute the 'active mirror' or VECSEL chip. The cavity with an extension in the centimeter range is completed by a high-reflectivity external mirror, which is also used for the out-coupling of the laser emission. The VECSEL chip is mounted on a heat sink which typically consists of a diamond heat spreader on top of a copper block. The QWs are optically pumped using commercially available high-power pump sources. Figure 1 shows a simple generic VECSEL layout.

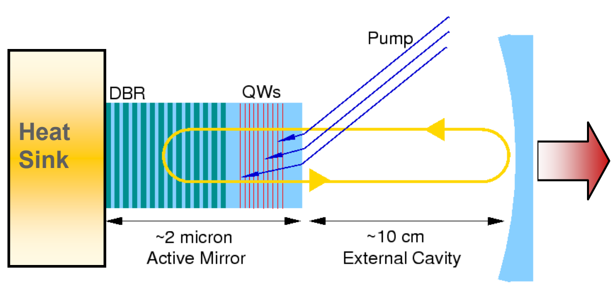

Figure 1. Schematic layout of a VECSEL device showing the QW structure grown on a distributed Bragg reflector (DBR) mirror stack consisting of quarter-wavelength thick layers of alternating semiconductor materials with high and low refractive index. Together, the DBR and the quantum wells constitute an 'active mirror'. The spacing between the typically 8 to 12 quantum wells is chosen to match half the wave length of the desired laser emission, constituting the resonantly periodic gain medium. The structure is pumped using external optical sources. Lasing is achieved by using an external high-reflectivity (out coupling) mirror to form a closed cavity. The generated heat is removed by a heat sink typically consisting of a diamond heat-spreader on a copper block.

Vertical External Cavity Surface Emitting Lasers (VECSELs) IV, edited by Jerome V. Moloney, Proc. of SPIE Vol. 8966, 896603 · © 2014 SPIE
CCC code: 0277-786X/14/$18 · doi: 10.1117/12.2036083

Besides the depicted linear cavity arrangement, also more elaborate geometries with so-called V-cavities or even more complicated structures are in practical use.

A wide variety of semiconductor materials can be used as the VECSEL gain medium allowing for lasing at many desirable wave lengths [2]. To further extend this range, one uses intracavity frequency up-conversion with suitable nonlinear crystals. Since VECSELs are optically pumped, one can realize close to circular beam profiles. Furthermore, the emission intensity scales with the pumped area such that high-power performance is possible. The wide range of envisioned VECSEL applications includes large-area projection, displays in automobiles, laser television, welding, micromachining, nonlinear microscopy, laser-induced breakdown spectroscopy, underwater photonics, and the realization of powerful THz emitters.

2. MICROSCOPIC APPROACH

In many ways, the VECSEL can be considered a physicist's dream system since virtually all aspects can be well-controlled experimentally and – at least in principle – computed theoretically. It all starts from the carrier generation via optical absorption of the pump beam in energetically high states well above the band gap. These carriers then relax into energetically lower states via carrier-carrier and carrier-phonon scattering. Both processes lead to the redistribution of the carrier populations into Fermi-Dirac functions. Since the Coulomb scattering conserves the total electronic energy, it leads to the establishment of a carrier specific electronic temperature. Through the phonon coupling, the electron-hole system loses energy to the lattice which leads to carrier cooling and lattice heating. All of these processes happen within the QWs and barriers. However, the heat is subsequently also transferred into the surrounding material, into the Bragg mirror, and from there into the heat sink. These heat-spreading effects are governed by classical drift and diffusion processes.

For too strong pumping, or if the pump energy is too close to the band gap, the filling of the carrier states leads to absorption bleaching, which renders the pumping inefficient. The degree of this Pauli blocking depends on the interplay between the generation of carriers and their subsequent relaxation into the unpumped, energetically lower states. The relaxed carriers then contribute to the QW gain, which directly depends on the detailed carrier distribution functions. Carriers are removed from the system via the desired stimulated recombination, by the unwanted but intrinsically unavoidable spontaneous emission, and by nonradiative (defect, Auger and intersubband) recombination processes. In order to treat all these effects correctly, one systematically has to account for the carrier Coulomb and phonon-scattering processes as well as their interactions with the light fields, i.e., the pump beam and the generated laser emission.

We treat the optically excited semiconductors as fully quantum-mechanical many-body systems whose properties are governed by the Coulomb interaction and coupling between charge carriers, photons, and phonons [3,4]. Hence, the total Hamiltonian contains the band structure part H_0, the light-matter interaction H_{lm}, the Coulomb-interaction H_{Coul} among the charge carriers, as well as the coupling to phonons,

$$H = H_0 + H_{\mathrm{lm}} + H_{\mathrm{Coul}} + H_{\mathrm{phon}}.$$

Since the system of electronic excitations has overwhelmingly many degrees of freedom, an attempt to solve the Schrödinger equation for the many-body wave function is not feasible with current computational resources. Therefore, we choose the alternative, quantum-dynamic approach based on the Heisenberg equations of motion.

Evaluating the commutators with the total Hamiltonian H, we derive the equations of motion for the relevant operator combinations. Focusing on the electronic excitations governing the response of the QW gain medium in the VECSEL systems, we need to compute the carrier distributions and the optically induced polarization (induced dipole density) whose expectation value enters Maxwell's wave equation as a source. With this input, we can then evaluate the electromagnetic field of the full system and determine, e.g., absorption and gain properties.

The microscopic polarization and its complex conjugate are the off-diagonal elements of the reduced single-particle density matrix. The diagonal elements are the electron and hole state-occupation probabilities, i.e., the carrier distribution functions. The dynamic equations for these single-particle quantities couple to two-particle correlations (doublets) due to the interaction parts of the Hamiltonian. Since the equations for the doublets involve three-particle quantities (triplets) which then couple to quadruplets etc., we encounter the infinite equation hierarchy, which is characteristic for quantum-mechanical many-body problems.

Schematically, the equation of motion for the expectation value <*N*> of an *N*-particle operator has the form

$$i\hbar\frac{\partial}{\partial t}\langle N\rangle = F\big[\langle N\rangle\big] + I\big[\langle N+1\rangle\big]$$

Here, *F*[<*N*>] describes the mean-field (Hartree-Fock) contributions, whereas the many-body interactions lead to a coupling to <*N*+1>-particle correlations, symbolically denoted by the functional *I*[<*N*+1>]. The generic structure of the dynamic equation for <*N*> is typical of a many-body system with single-particle contributions and pairwise particle interactions. The ever-rising hierarchy couples the *N*-particle expectation values to the *N+1*-particle correlations.

Since we want to treat all the correlations of a given order systematically with the same level of accuracy, we decompose all expectation values into singlets, correlated doublets, correlated triplets and higher order correlations. As symbolically shown in Fig. 2, we identify the *correlated parts* (shaded areas in Fig. 2) as the full expectation values minus their lower-order factorizable ingredients. This approach is based on the idea that any given <*N*>-particle quantity can be expressed in terms of a consistent factorization (see Fig. 2) into:

- independent single particles (singlets),
- correlated pairs (doublets),
- correlated three-particle clusters (triplets),
- …………..,
- correlated *N*-particle clusters.

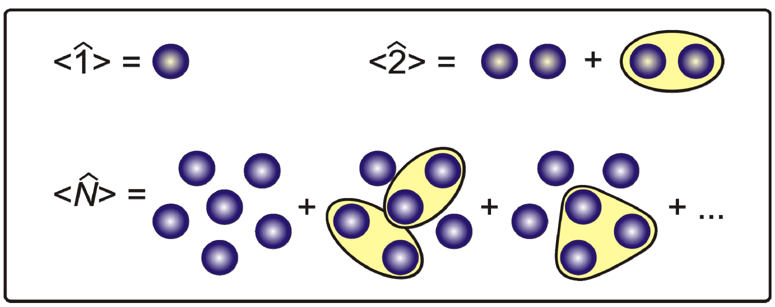

Figure 2. Schematic decomposition of N-particle expectation values for N= 1, 2, and 6. The systematic factorization involves singlets (spheres) and correlated clusters (shaded areas). The explicit scheme includes all possible factorizations based on the indistinguishability of the analyzed Fermions or Bosons.

In many ways, the different clusters can be considered as moments and cumulants (e.g., variance and kurtosis) of quantum-statistical distributions. Since the relatively high electron-hole-pair density in a VECSEL induces strong screening, dephasing, and particle scattering effects, we expect higher-order correlations to be of reduced significance. We therefore truncate the equation hierarchy with the help of the cluster-expansion method. As relevant singlet contributions, we treat the electron and hole occupation probabilities and the optical polarization. Doublets include exciton populations, photon-assisted polarizations etc.

This correlated-cluster expansion and truncation procedure allows us to account for all the important physical properties of our system and to avoid all the notorious problems that typically arise in *ad-hoc* approximations. In contrast to such unsystematic treatments, our approach assures the consistent evaluation of all the contributions at the same correlation level. In particular, we fully include the intrinsic balancing effects such as the compensation of the excitation-induced excitonic blue shift by the red shift of the band gap or the cancellations between diagonal and off-diagonal contributions in the microscopic dephasing analysis.

The cluster truncation casts the equation hierarchy into a closed form [4]. However, due to the very large number of quantum states in the semiconductor system, one still has to deal with extended sets of integro-differential equations. After the integral discretization, we are left with huge numbers (often many hundreds of millions) of coupled ordinary differential equations (ODEs). The efficient choice of the discretization scheme and the numerical treatment of the ODEs constitute significant challenges in their own right. The successful numerical implementation requires advanced computation strategies and dedicated high-performance hardware.

3. QUANTUM DESIGN OF VECSELS

For the design and optimization of real VECSELs [5], we have to implement a full multiband approach in order to account for the quantum confinement and strain effects in the QWs. Using the appropriate band structure theory, we will compute the relevant single-particle dispersions in H_0 of Eq. (1) for the particular heterostructure system under investigation. In most cases, we will apply the multiband k·p approach with optimized parameters obtained from detailed theory-experiment comparisons or from an analysis of density-functional calculations. We use the k·p wave functions to evaluate the interband dipole and Coulomb matrix elements in $H_{\rm lm}$ and $H_{\rm Coul}$ of Eq. (1), respectively. In order to account for the dielectric environment, we will adopt our filter function scheme to relate the emission from a free-standing QW to the full microcavity output.

Typically, one uses around 10 QWs as the resonantly periodic VECSEL gain medium. The precise number is a compromise between the pump power needed to achieve inversion (i.e., the laser threshold) and the gain provided by the QWs. Since the laser light propagates perpendicular to these wells, there is not much round-trip amplification. Hence, one has to make sure that the available gain is optimally utilized, i.e., the spectral gain maximum and the cavity mode have to be very well aligned under lasing conditions.

In this context, the thermal problems need particular consideration. Heat is generated via the so-called quantum defect caused by the excess energy pumped into the system when generating carriers at frequencies well above the lasing frequency. Those carriers have to relax into lower states via carrier scattering and phonon emission before they can contribute to the lasing. Furthermore, the nonradiative carrier loss processes significantly increase the thermal carrier energy. Part of this heat is removed by providing a proper heat sink. To account for this effect, we complement our microscopic equations with classical drift-diffusion models for the heat transfer from the optically pumped active region to the lattice and the heat sink.

In comparison to most standard semiconductor-laser models, the main improvements of our microscopic approach are:

⇒ We do not assume parabolic bands with simple effective masses. Instead, we perform multiband k·p band structure calculations including the effects of quantum confinement and strain in the particular heterostructure arrangement. We use the resulting band dispersions as single-particle energies and the wave functions to evaluate all the dipole- and Coulomb-coupling matrix elements needed.

⇒ We systematically include the Coulombic interaction of the charge carriers. Already at the singlet (Hartree-Fock) level, these interactions lead to effects like the density and temperature dependent renormalization of the semiconductor band gap and the interband enhancement. Band gap renormalization leads to significant spectral shifts of the gain whereas interband (excitonic) enhancement reshapes the spectra.

⇒ We do not use a dephasing (T_2) time. As a matter of fact, one obtains the wrong (Lorentzian) line shape for the individual transitions if one approximates the microscopic polarization damping processes in such a simple way. One of the prominent consequences of these incorrect line shapes is the unphysical appearance of optical absorption energetically below the gain spectra. In our modeling, we use the set of microscopic equations resulting from our cluster-expansion scheme. This way, we automatically include the particle scattering and *excitation induced dephasing* processes. Combining the results obtained with the solution of Maxwell's wave equation, we can thus evaluate the optical absorption/gain and refractive-index spectra including all relevant confined subbands and barrier states of the heterostructure. With this approach, we eliminate the long standing semiconductor laser line shape problem. This enables us to reliably predict gain/absorption and refractive index spectra. *Remarkably, dynamic scattering processes occurring on tens to hundreds of femtosecond time scales profoundly modify the CW semiconductor optical response.*

⇒ We eliminate the heuristic carrier lifetime approximation. Instead, we compute the spontaneous electron-hole recombination processes by solving the quantum semiconductor luminescence equations (SLE) for the multiband semiconductor systems.

⇒ We abandon the traditional models which reduce the Auger losses to a simple cubic power-law dependence of the loss current on the carrier density. Instead, we use our full microscopic many-body theory for the evaluation. The resulting equations involve high-dimensional momentum-state integrals and sums over the multitude of different band (subband) combinations. We have to evaluate all the different scattering matrix elements as well as the microscopic in- and out-scattering probabilities.

⇒ The carrier capture from states located in the barriers and/or energetically high quantum well states is calculated explicitly by evaluating the underlying microscopic scattering processes. This eliminates the otherwise required phenomenological carrier capture times which simulate the refilling of states contributing to the optical gain near the bottom of the quantum well by assuming carrier relaxation that is independent of the subband, in-plane momentum of states and, usually, temperature and operating density. The underlying scattering equations are of similar complexity as those involved in the dephasing of the polarizations and the Auger scattering.

Due to the complex interplay of the heat generation and dissipation processes, it is *a priori* not known, at which effective temperature the system will operate, if it works at all. To make matters worse, the temperature of the carrier plasma, i.e., the electronic temperature, and the temperatures of the host lattice and of the heat sink are generally all different and depend on the operating conditions. Since semiconductor gain/absorption, radiative and nonradiative losses as well as cavity resonance all change with temperature, one directly sees the strength of our approach, which self-consistently evaluates all of these properties together with the thermal analysis.

4. NONEQUILIBRIUM ASPECTS IN VECSEL MODELING

Under many conditions, it is not sufficient to approximate the carriers in VECSELs by a quasi-equilibrium system, instead so-called nonequilibrium effects become important. One nonequilibrium situation is realized under high-power laser-operation conditions, where the stimulated carrier recombination strongly depletes those states that are resonant with the laser emission wavelength.

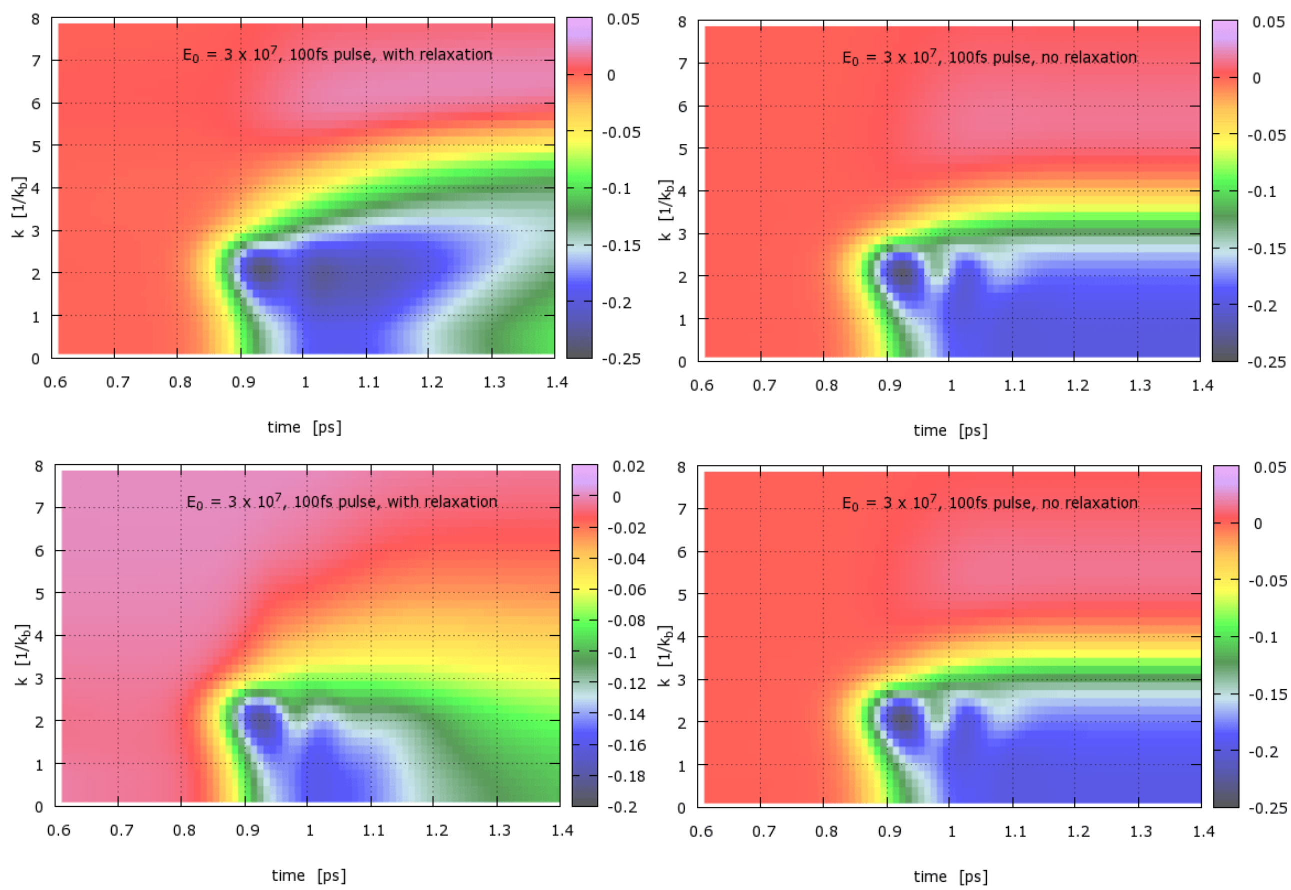

Figure 3. Deviation from the equilibrium carrier distribution caused by a 100fs pulse centered at 1ps and having a central frequency near the maximum of the gain. Top: lowest electron subband. Bottom: lowest hole subband. Left: carrier redistributions due to carrier scatterings during the pulse are included. Right: without carrier scatterings. Simulation for a quantum well of a VECSEL operating at 1040nm, a heat sink temperature of 300K and an equilibrium density that is typical for laser operation of this device (5×10^{12} cm^{-2}).

The state-selective rapid interband transitions lead to kinetic hole-burning, i.e. nonequilibrium deviations of the actual carrier distribution from quasi-equilibrium Fermi-Dirac distributions even in steady-state operation. The depth and extend of these kinetic holes is ultimately determined by the balance between the stimulated carrier removal and the replenishing of the carrier populations via carrier-carrier and carrier-phonon scattering. Other important aspects are the overall carrier pumping (optical or though current injection) and the heat balance. The pumping adds carriers in energetically higher states from where they have to loose energy before they contribute to the lasing. As discussed above, this energy loss leads to carrier and lattice heating, requiring sophisticated thermal balancing to maintain stationary high-power operation.

Another important nonequilibrium situation concerns the ultra-short pulse generation in VECSELs. To determine the ultimate limit for the shortest possible pulse duration in a semiconductor medium has intrigued and challenged physicists for many decades. The available gain bandwidth of semiconductor heterostructures suggests that it should be possible to generate ultrashort optical pulses in the regime of few femtoseconds or less. However, state-of-the-art experimental verifications so far are hardly able to go much below the regime of 100s of fs.

For the microscopic modelling of the VECSEL nonequilibrium effects, we use the semiconductor Bloch equations (SBE), i.e. the coupled equations of motion for the carrier occupation probabilities of the different band states and the optically induced interband polarizations between those states [3,4]. To obtain some basic insights into the significance of nonequilibrium features, we are numerically integrate the SBE for a situation typical for mode locked pulsed operation. The quantum wells are inverted and the distributions are in thermal equilibrium. Then the system is hit by a short, intense light pulse with a central frequency corresponding to the energy of maximum quantum well gain. This pulse depletes the carrier inversion due to stimulated emission leading to a so-called spectral hole in the distributions. If the pulse is strong enough, it will eventually lead to a distribution in the well for which the system becomes transparent. In an ideal system with equal electron and hole masses, a single frequency pulse and no carrier re-distributions due to scattering, the remainder of the pulse would pass through the well without further modifications of the system. However, as can be seen in Figure 3, in a realistic situation the pulse causes further changes in the distributions due to changes from absorptive- to gain-behavior in a Rabi-flopping manner.

Without carrier re-distributions due to electron-electron and electron-hole scattering, the distributions become static once the pulse has passed the system. Eventually, the lost carriers will be re-filled by the pump light and subsequent carrier relaxation from the barriers to the wells (barrier-pumping is assumed here). However, this happens on a rather slow timescale of typically ten(s) of picoseconds.

Taking into account the carrier scatterings explicitly reveals a far more complex dynamic. As mentioned, the pump-injection of carriers happens on a picosecond-timescale. This involves carrier transitions between different subbands which is slow due to the rather large required energy transfer. However, Coulomb scattering within each subband takes place on a much faster timescale of only ten(s) of femtoseconds. This leads to significant modifications already during the presence of the light-pulse. Carriers from higher and lower momentum states re-fill the spectral hole at the lasing frequency during and after the pulse. Eventually, this leads to a hot equilibrium distribution that is cooled down on a slower timescale by phonon scatterings.

The intra-subband scattering also allows for the pulse to deplete more carriers due to stimulated emission than would be possible otherwise (se Fig. 4). This means that the amplification of the pulse is also much stronger than one would assume otherwise. The scattering re-fills the states near the center frequency of the pulse while the pulse is still there and the pulse can stimulate these additional carriers to recombine. Since the intraband scattering time is on the scale of tens of femtoseconds, this effect becomes more pronounced the longer the pulse is. In our case, for a 15fs pulse it only enhances the total amount of carriers lost to stimulated emission by a few tens of percent. For a 100fs pulse it almost doubles the amount.

This simulation clearly demonstrates the underlying microscopic complexity of a typical laser situation. The microscopic scatterings dramatically alter the distribution functions already during the presence of a femtosecond pulse. This will modify the amplification of the pulse – its overall amplification as well as its spectral dependence. In turn, this will lead alter the phase changes experienced in the quantum well medium. Overall, these processes have to be taken into account seriously if one attempts to model mode locked VECSELs or tries to determine optimal solutions like, the shortest possible pulse, the shortest possible pulse repetition or the strongest possible pulses.

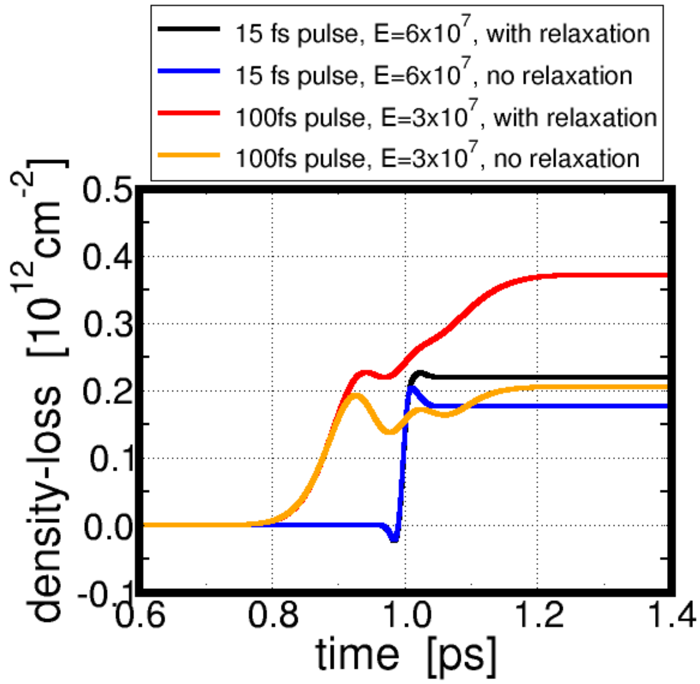

Figure 4. Density loss due to stimulated emission for the numerical experiment from Fig. 3 (red, orange) and for the same case but a pulse length of only 15fs and an adjusted pulse amplitude (E, in arb. Units) (black, blue). The density loss is much stronger, especially for a longer pulse, if carrier redistribution due to scatterings within the subbands during the pulse are taken into account ('with relaxation').

Acknowledgements: This work is supported by AFOSR (grant FA9550-10-1-0064) and by the German Science Foundation (DFG: GRK1782).

References[1]M. Kuznetsov *et al.,* IEEE J. Sel. Top. Quantum Electron.**5**, 561 (1999).
[2] For reviews see, e.g., U. Keller and A. C. Tropper, Phys. Rep. **429**, 67 (2006); N. Schulz *et al.*, Laser Photon. Review **2**, 160 (2008); S. Calvez *et al.*, Laser Photon. Review **3**, 407 (2009) and references therein.
[3]H. Haug and S. W. Koch, *Quantum Theory of the Optical and Electronic Properties of Semiconductors*, fifth ed., World Scientific Publ., Singapore (2009).
[4]M. Kira and S. W. Koch, Prog. Quantum Electron. **30**, 155 (2006).
[5]J.V. Moloney, J. Hader, and S.W. Koch, Laser Photon. Review **1**, 24 (2005) and references therein.